MOLECULAR AND CELLULAR BIOLOGY, Oct. 2006, p. 7451–7465 Vol. 26, No. 20
0270-7306/06/$08.00+0 doi:10.1128/MCB.00684-06

An *hpr1* Point Mutation That Impairs Transcription and mRNP Biogenesis without Increasing Recombination▽

Pablo Huertas, María L. García-Rubio, Ralf E. Wellinger, Rosa Luna, and Andrés Aguilera*

Departamento de Genética, Facultad de Biología, Universidad de Sevilla, Avd. Reina Mercedes 6, 41012 Sevilla, Spain

Received 20 April 2006/Returned for modification 13 June 2006/Accepted 4 August 2006

THO/TREX, a conserved eukaryotic protein complex, is a key player at the interface between transcription and mRNP metabolism. The lack of a functional THO complex impairs transcription, leads to transcription-dependent hyperrecombination, causes mRNA export defects and fast mRNA decay, and retards replication fork progression in a transcription-dependent manner. To get more insight into the interconnection between mRNP biogenesis and genomic instability, we searched for *HPR1* mutations that differentially affect gene expression and recombination. We isolated mutants that were barely affected in gene expression but exhibited a hyperrecombination phenotype. In addition, we isolated a mutant, *hpr1-101*, with a strong defect in transcription, as observed for *lacZ*, and a general defect in mRNA export that did not display a relevant hyperrecombination phenotype. In *THO* single-null mutants, but not in the *hpr1* point mutants studied, THO and its subunits were unstable. Interestingly, in contrast to hyperrecombinant null mutants, *hpr1-101* did not cause retardation of replication fork progression. Transcription and mRNP biogenesis can therefore be impaired by THO/TREX dysfunction without increasing recombination, suggesting that it is possible to separate the mechanism(s) responsible for mRNA biogenesis defects from the further step of triggering transcription-dependent recombination.

Gene expression requires the correct coupling of transcription to mRNA processing and export (7, 17, 30, 31). The final outcome of transcription is a ribonucleoprotein particle (mRNP) consisting of an mRNA molecule bound to proteins, which later function in export, mRNA surveillance, and translation. Transcription and assembly of the mRNP are tightly coordinated with the export of mRNA (42). A number of proteins have been identified that are important for the correct assembly of export-competent mRNP particles, including the THO complex, composed of Tho2, Hpr1, Mft1, and Thp2, as identified in *Saccharomyces cerevisiae* (9). THO has also been purified from humans and *Drosophila*, in which Hpr1 and Tho2 homologues are present (32, 40). In yeast and humans, it has been shown that THO is part of the TREX complex, which includes the Sub2/UAP56 and Yra1/Aly mRNA export factors (40). Functional connections between THO and the Sub2 and Yra1 export factors have been shown by synthetic lethal phenotypes of double mutants and by multicopy suppression (11, 19, 40).

Null mutants of the THO complex are impaired in transcription elongation (8, 23, 36). Additionally, these mutants exhibit a plethora of phenotypes, including transcription-dependent hyperrecombination (2), nuclear mRNA retention (40), and fast mRNA degradation (22, 46), as well as synthetic lethality in combination with mutations affecting transcription elongation such as *spt4* (35) and with RNA export mutations such as *mex67-5* and *yra1-1* (19, 40). Altogether, these data suggest that THO plays a crucial role in mRNP metabolism at the interface between transcription and mRNP export. Mutants with changes affecting the Sub2-Yra1 component of TREX, the Mex67-Mtr2 mRNA export factor, the Nab2 hnRNP, or the Thp1-Sac3-Sus1 RNA export complex exhibit transcription and genetic instability phenotypes similar to those of THO mutants (12, 14, 19).

The THO complex is exclusively recruited to transcribed chromatin (20, 40, 46). Recruitment of the Sub2 and Yra1 components of the THO/TREX complex to transcribed DNA is partially dependent on THO (46). In contrast to THO, binding of Sub2 to transcribed chromatin is RNA dependent (1). The relevance of THO in the early steps of mRNP biogenesis is supported by the observation that transcription impairment in *hpr1*Δ mutants is suppressed if the nascent mRNA is self-cleaved by an artificially engineered hammerhead ribozyme. In these mutants, the nascent mRNA can form RNA-DNA hybrids (R loops) linked to both impairment of transcription and transcription-associated recombination (18). The observation that depletion of the vertebrate ASF/SF2 splicing factor in chicken DT40 cells and human HeLa cells also leads to genomic instability linked to R loop formation (21) indicates that a number of mRNA processing enzymes may have a role in preventing RNA-dependent structures that trigger genome instability. Our current view is that the THO complex participates in cotranscriptional assembly of export-competent mRNP during transcription elongation and contributes to the prevention of the RNA from forming structures that hamper transcription and could compromise genome stability (3).

Despite the link between impaired transcription and hyperrecombination in THO mutants, it is not clear whether impaired gene expression by itself is sufficient to induce hyperrecombination or whether hyperrecombination is possible in the absence of impaired gene expression. Thus, we searched for THO mutants compromised in gene expression that did not affect genetic integrity and vice versa. Hyperrecombination

* Corresponding author. Mailing address: CABIMER, Av. Americo Vespucio s/n, 41092 Seville, Spain. Phone: 34 954 468372. Fax: 34 954 461664. E-mail: aguilo@us.es.

▽ Published ahead of print on 14 August 2006.

TABLE 1. Yeast strains used in this study

Strain	Genotype	Source or reference
W303-1A	*MAT***a** *ade2-1 can1-100 his3-11,15 leu2-3,112 trp1-1 ura3-1*	R. Rothstein
AYW3-1B	*MAT*α *ade2 can1-100 his3 trp1 ura3 leu2-k*::*ADE2-URA3*::*leu2-k*	13
U768-4C	W303-1A *hpr1*Δ::*HIS3*	R. Rothstein
SChY58a	W303-1A *hpr1*Δ::*KAN*	S. Chávez
WH101-1A	W303-1A *hpr1-101*	This study
WH103-1A	W303-1A *hpr1-103*	This study
BSU-S2T-6D	*MAT***a** *ade2-1 leu2 hpr1*Δ::*HIS3 SUB2-TAP*	19a
LAU3-10A	*MAT***a** *ade2-1 his3-11,15 trp1-1 ura3-1 leu2-k*::*ADE2-URA3*::*leu2-k hpr1*Δ::*KAN*	This study
LAU3-10D	*MAT*α *ade2-1 his3-11,15 trp1-1 ura3-1 leu2-k*::*ADE2-URA3*::*leu2-k*	This study
WMC1-1A	W303-1A *mex67-5*	19
WMH1	*hpr1*Δ::*KAN mex67-5* isogenic to W303-1A and transformed with pRS316-HPR1	This study
WWT2T	W303-1A *THO2-TAP*	19a
WTT3-4A	W303-1A *THO2-TAP hpr1-101*	This study
WTT3-4C	W303-1A *THO2-TAP hpr1*Δ::*KAN*	This study
STT2	W303-1A *THO2-TAP sub2*Δ::*HIS3*	19
MTT1	W303-1A *THO2-TAP mft1*Δ::*KAN*	S. Jimeno
WTT4-5C	W303-1A *THO2-TAP hpr1-103*	This study
WHYL.2A	W301-1A *hpr1*Δ::*HIS3 GAL1pr*::*YRL454*	19a

mutations that did not have a significant effect on transcription were not found. Instead, we isolated a new allele, *hpr1-101* (L586P), which causes a strong decrease in transcript accumulation but does not show a relevant hyperrecombination phenotype. The in vivo stability of THO and its subunits was strongly reduced in THO-null mutants such as *hpr1*Δ but not in *hpr1* point mutants. The absence of associated hyperrecombination seems to be due to the fact that, in contrast to *hpr1*Δ, transcription impairment in *hpr1-101* does not hamper replication fork progression. Our results indicate that THO dysfunction can cause transcription defects that are not linked to impairment of replication fork progression, opening the possibility that THO links optimal mRNP biogenesis with transcription elongation, apart from its effect on genomic integrity.

MATERIALS AND METHODS

Strains and plasmids. The strains used in this study are listed in Table 1. All of the strains are isogenic to W303-1A, except LAU3-10A and LAU3-10D, which are congenic segregants from a SChY58A × AYW3-1B cross. Strains WH101-1A and WH103-1A, isogenic to W303-1A but harboring the *hpr1-101* and *hpr1-103* alleles in the *HPR1* chromosomal locus, were obtained by gene replacement in SChY58a (*hpr1*Δ::*KAN*). Plasmids pRS313, pRS316 (38), YCp70, YCpA13 (4), pRS314GLlacZ (15), YEp351-SUB2, pCM184-LAUR (19), pRS316-GAL1lacZ, pSCh202, pSCh204, pSCh206 (8), pPHO5-Rib$^+$-lacZ (Rib$^+$), pPHO5-rib^m-lacZ (rib^m), pGL-Rib$^+$, pGL-rib^m (18), and pRWY005 (43) have been described previously. Plasmid pRS313-GZ was constructed by cloning the *GAL1pr*::*lacZ* fusion from pRS316-GAL1lacZ into pRS313 in vivo as previously described (29). pRS316-HPR1 was obtained by cloning the 6.55-kb HindIII *HPR1* fragment from YCpA13 into the HindIII site of pRS316. Plasmids YCphpr1-101 to YCphpr1-104 were obtained by in vivo cloning of linear mutagenized *HPR1* PCR fragments into YCp70 in yeast strain LAU3-10A as described below.

New *hpr1* alleles obtained by random mutagenesis. In vitro mutagenesis of *HPR1* was performed according to reference 27, with some modifications. PCR amplification of *HPR1* was done under suboptimal conditions with 3.25 mM $MgCl_2$, 0.25 mM $MnCl_2$, 0.2 mM dTTP, 0.2 mM dGTP, 0.2 mM dCTP, 0.04 mM dATP, and 1.75 U of Expand High Fidelity *Taq* polymerase (Roche). YCpA13 (1 μg) was used as the template, and the oligonucleotides 5′ GCCACGTTTGTT TACTCG 3′ and 5′ CTATCATCCAACGCTTCC 3′ were used as primers. The LAU3-10A strain (*hpr1*Δ), previously transformed with pRS313-GZ, was cotransformed with the purified, PCR-mutagenized *HPR1* mixture and the linear BamHI-XbaI fragment of YCpA13, which corresponds to YCp70 carrying 200 bp of *HPR1* flanking sequences on each side. In vivo recombination between the PCR-induced *hpr1* alleles and the linear vector led to formation of the YCphpr1 plasmids in the cells. Transformants thus obtained were plated on synthetic complete (SC) medium without histidine and leucine containing limited amounts of adenine (1.5 mg/liter) for visualization of red sectors resulting from recombination of the chromosomal *leu2-k*::*ADE2-URA3*::*leu2-k* repeat system. Colonies were then replicated onto SC without histidine and leucine containing 2% galactose to allow expression of the *GAL1pr*::*lacZ* fusion. On the following day, a solution containing 0.25 M phosphate buffer (pH 7.5), 0.1% sodium dodecyl sulfate (SDS), 400 μg/ml 5-bromo-4-chloro-3-indolyl-β-D-galactopyranoside (X-Gal), and 0.5% agarose was added and β-galactosidase activity was scored by blue color formation after 2 h at 30°C. Colonies transformed with either YCpA13 or YCp70 were used as positive (wild type) or negative (*hpr1*Δ) controls, respectively.

Purification of the THO complex and analysis of its subunits. The THO complex was purified by using the C-terminally tandem affinity purification (TAP) epitope-tagged Tho2 protein and following standard procedures (33) and using specifications previously reported (19). Mft1 was detected by Western analysis of purified THO complexes previously separated by 10% SDS-polyacrylamide gel electrophoresis (PAGE) and transferred to nylon membranes. After treatment with phosphate-buffered saline containing 0.1% Tween 20 and 5% milk, proteins were detected with anti-Mft1 antibody and peroxidase-conjugated goat anti-rabbit immunoglobulin G (IgG). Blots were washed with phosphate-buffered saline–0.1% Tween 20 and developed by enhanced chemiluminescence reactions (Amersham). The Tho2-TAP epitope fusion was detected in whole cell extracts with peroxidase antiperoxidase (PAP; Sigma) antibody by following the manufacturer's instructions as described previously (19).

2D gel analysis of replication intermediates. Cells were grown overnight to an optical density at 600 nm of 0.2 to 0.3 in SC medium containing 1% glycerol-lactate and 1% raffinose as a carbon source. After bringing the culture to 2% galactose, cells were grown for another 3.5 to 4 h prior to DNA isolation. DNA of 100 ml of cells was isolated with cetyltrimethylammonium bromide (44), dissolved in a final volume of 100 μl of Tris-EDTA, and stored at 4°C. Prior to analysis, 50 μl of DNA was double digested with SmaI-SacI. After digestion, DNA was precipitated and subjected to two-dimensional (2D) gel electrophoresis as described previously (6), with the following modifications. DNA was separated for 20 h in the first dimension on a 0.5% agarose gel at 1 V/cm and for 14 h in the second dimension on a 1.2% agarose gel at 4 V/cm and 4°C in the presence of 0.3 μg/ml ethidium bromide. After alkaline transfer of the DNA onto a Hybond-N$^+$ membrane, the membrane was hybridized against a ^{32}P-labeled 1.2-kb fragment obtained by PCR covering *ARS1* and part of the 3′-*lacZ* gene. Membranes were exposed on a Fuji 3600 Phosphorimaging system and analyzed with the imaging software supplied.

ChIP. Recruitment of Sub2, Tho2, and RNAPII to chromatin was determined by chromatin immunoprecipitation (ChIP) analyses on the endogenous *PMA1* gene in yeast strains containing a 5′-end TAP epitope-tagged version of either the *SUB2* or the *THO2* gene inserted at its chromosomal locus, as previously described (16). Briefly, immunoprecipitations were performed with Ig-Sepharose for TAP epitope-tagged proteins or with anti-Rpb1-CTD monoclonal antibody

8WG16 (Berkeley Antibody Company) and protein A-Sepharose for RNA polymerase II (RNAPII). The GFX purification system (Amersham) was used for the last DNA purification step. We used 20- to 27-bp oligonucleotides for PCR amplification of *PMA1* sequences. For Tho2 recruitment, we amplified two fragments, localized at positions 292 to 321 and 2273 to 2242, whereas for Sub2 and RNAPII recruitment, we only amplified the 2273-to-2242 fragment. In both cases, we used the PCR of the intergenic region at positions 9716 to 9863 of chromosome V as a negative control. The PCR products obtained were electrophoresed in a 15% acrylamide gel, stained with ethidium bromide, and quantified in a Fuji FLA-3000. The relative abundance of each DNA fragment was calculated as the ratio of each DNA fragment to the intergenic-region quantification results of the precipitated fractions normalized with respect to the corresponding ratios of the input fractions.

For analysis of RNAPII processivity, a strain harboring either YLR454 or *lacZ* under the control of the *GAL1* promoter was used (23). RNAPII abundances at different positions of the genes were assayed as indicated, by using ChIP with anti-Rpb1-CTD monoclonal antibody 8WG16 and protein A-Sepharose as previously described (23). We used 20- to 30-bp oligonucleotides for PCR amplification of two fragments of YLR454, positions 3 to 43 and 7621 to 7674; of two fragments of *lacZ*, positions 715 to 1025 and 2247 to 2467; and of the 9716-to-9863 intergenic region of chromosome V that was used as a control. Real-time quantitative PCR was performed with SYBR green dye in the 7500 Real Time PCR system of Applied Biosystems by following the manufacturer's instructions.

Miscellanea. Recombination frequencies were calculated as previously described (18). For each genotype, the recombination frequencies are given as the average and standard deviation of the median recombination value obtained from two or three different transformants with 6 to 12 independent colonies per transformant. β-Galactosidase and phosphatase assays and Northern analyses were performed according to previously published procedures (18). mRNA export assays were performed by in situ poly(A)$^+$ RNA localization with a synthetic digoxigenin-labeled oligo(dT)$_{20}$ as previously described (5, 14).

RESULTS

Isolation of *hpr1* mutations with differential effects on gene expression and genetic instability. Mutagenic PCR-generated *hpr1* alleles were cloned into the YCp70 plasmid by in vivo homologous recombination (see Materials and Methods). *hpr1* mutations that differentially affected gene expression and recombination were screened by a color assay based on the chromosomal *leu2-k*::*ADE2-URA3*::*leu2-k* direct-repeat construct (4). With this construct, wild-type cells form white colonies (Ade$^+$) whereas *hpr1* cells form red-sectoring colonies (Ade$^+$ Ade$^-$). Defects in gene expression were determined with a *GAL1pr*::*lacZ* fusion construct which results in a dark blue color in expression-competent wild-type colonies and a light blue color in expression-deficient *hpr1* mutant colonies. Screening of 5,346 transformant colonies permitted the identification of four *hpr1* mutants (*hpr1-101* to *hpr1-104*) which, upon subsequent analyses, were verified as being preferentially hyperrecombinant or defective in *lacZ* expression. The *hpr1* alleles were sequenced, and the mutations responsible for the amino acid changes of each allele were determined (Fig. 1A). *hpr1-101* harbors two point mutations, but only one (L586P) leads to amino acid substitution. Interestingly, although the primary sequence of the Hpr1 protein is not particularly conserved, this mutation lies in a highly conserved region (Fig. 1B). *hpr1-102* has a −1 frameshift that leads to a premature stop codon and a carboxy-terminally truncated Hpr1 protein. *hpr1-103* and *hpr1-104* harbor multiple point mutations leading to 12 and 6 amino acid substitutions, respectively.

Next, recombination frequencies and β-galactosidase activities were determined in a LAU3-10A *hpr1*Δ strain carrying the *leu2-k*::*ADE2-URA3*::*leu2-k* and *GAL1pr*::*lacZ* systems, respectively, and transformed with the YCp70::*hpr1* series of plasmids (*hpr1-101* to *hpr1-104*), YCpA13 (*HPR1*), or the empty vector YCp70 (*hpr1*) (Fig. 1C). *hpr1*Δ cells display a strong reduction in β-galactosidase activity (a 25-fold decrease) that correlates with a strong increase in recombination (773-fold above the wild-type level). Like *hpr1*Δ cells, *hpr1-101* and *hpr1-102* cells exhibit a significant reduction in β-galactosidase activity (4.3- and 6.7-fold decreases, respectively) which, in contrast to *hpr1*Δ, was accompanied by a weak increase in recombination (5- and 50-fold, respectively). Instead, β-galactosidase activity in *hpr1-103* and *hpr1-104* cells was poorly affected (1- to 2-fold decreases), while recombination values (239- and 567-fold above the wild-type level) were close to the values obtained in *hpr1*Δ. We therefore decided to further analyze *hpr1-101* and *hpr1-103* in order to understand the basis for the different phenotypes they produce.

***hpr1-101* causes a gene expression defect not associated with hyperrecombination, whereas *hpr1-103* affects both gene expression and recombination.** The strength of the gene expression defect and hyperrecombination phenotypes of *hpr1*Δ has been shown to be dependent on the DNA sequence (10). Thus, transcription through the *lacZ* bacterial gene is severely compromised in *hpr1*Δ and leads to strong hyperrecombination, but the transcription defect and hyperrecombination phenotypes are weak or barely detectable in other DNA sequences, such as that of *PHO5*. To understand the connection between the gene expression and recombination phenotypes observed in the *hpr1* point mutants, we further analyzed the most representative alleles, i.e., *hpr1-101* (strong gene expression defect and weak hyperrecombination) and *hpr1-103* (weak gene expression defect and strong hyperrecombination). Thus, we constructed isogenic strains harboring single chromosomal copies of *hpr1-101* (WH101-1A) and *hpr1-103* (WH103-1A) at the *HPR1* locus by gene replacement.

Recombination analysis in the L-*lacZ* system, containing *lacZ* flanked by *leu2* direct repeats, revealed that, compared to *hpr1*Δ (recombination 87-fold above the wild-type level), hyperrecombination was weak in *hpr1-101* (8-fold) and moderate in *hpr1-103* (20-fold) (Fig. 2A). Next, we analyzed recombination in the L-*PHO5* and GL-*lacZ* systems, the latter of which is the same as L-*lacZ* except that transcription is driven by the *GAL1* promoter. With either actively transcribed L-*PHO5* or GL-*lacZ* under repressive conditions (2% glucose), we obtained wild-type recombination levels in the L-*PHO5* and GL-*lacZ* systems in both *hpr1-101* and *hpr1-103*, respectively. These results indicate that hyperrecombination was transcription and sequence dependent in both mutants. In order to determine whether transcription impairment and hyperrecombination in these mutants are associated, we analyzed transcript levels in the same system used to measure recombination. Northern analysis showed similar *L-PHO5* transcript levels for all of the strains (Fig. 2B). Importantly, in the *hpr1-103* mutant the transcript levels of *lacZ* mRNA expressed from the L-*lacZ* system only reached 75 to 80% of the wild-type levels, which clearly differs from the β-galactosidase results obtained in the *GAL1pr*::*lacZ* system (Fig. 1C and data not shown). Thus, when transcription was analyzed in the same system in which hyperrecombination was detected, the *hpr1-103* mutant showed the same phenotypes as *hpr1*Δ, although to a lesser extent. As the L-*lacZ* and *GAL1pr*::*lacZ* systems differ in the length of the transcribed DNA sequence, it seems that

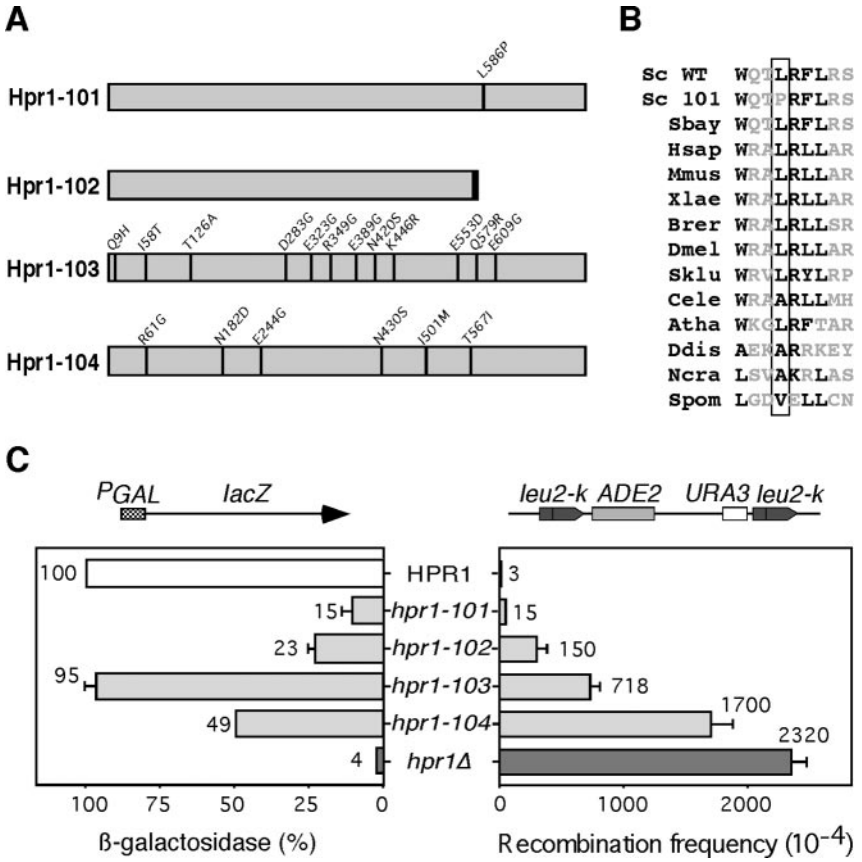

FIG. 1. Genetic characterization of *hpr1* point mutations that differentially affect transcription and recombination. (A) Schematic representation of the amino acid substitutions of the *hpr1* alleles studied. Mutations that change the amino acid sequence are represented as black bars. (B) Protein alignment of the region surrounding L586 in several Hpr1 orthologs. The Hpr1 protein sequences used belong to the followings organisms: *S. cerevisiae* wild type and *hpr1-101* mutant (Sc WT and Sc 101, respectively), *Saccharomyces bayanus* (SBay), *Homo sapiens* (Hsap), *Mus musculus* (Mmus), *Xenopus laevis* (Xlae), *Brachydanio rerio* (Brer), *Drosophila melanogaster* (Dmel), *Saccharomyces kluyveri* (Sklu), *Caenorhabditis elegans* (Cele), *Arabidopsis thaliana* (Atha), *Dictyostelium discoideum* (Ddis), *Neurospora crassa* (Ncra), and *Schizosaccharomyces pombe* (Spom). (C) β-Galactosidase activity and recombination frequencies of the LAU3-10A (*hpr1*Δ) strain containing the *leu2-k*::*ADE2-URA3*::*leu2-k* recombination system and transformed with pRS313-GZ (containing the *GAL1pr*:::*lacZ* fusion) and with either YCpA13 (*HPR1*), YCp-hpr1-101 to YCp-hpr1-104 (*hpr1-101* to *hpr1-104*), or the empty vector YCp70. The percentage of β-galactosidase activity with respect to the wild-type level (taken as 100%) is shown. Each value represents the average of two or three independent experiments. The recombination frequencies (10^{-4}) are averages of two to four median frequencies obtained from the same number of fluctuation experiments.

the *hpr1-103* effect on transcription was detectable in long DNA sequences. This is consistent with previous observations indicating that hyperrecombination is only observed in association with a detectable transcription defect (2).

RNAPII processivity is impaired in *hpr1-101* mutants. Since *hpr1-101* did not display a significant hyperrecombination phenotype compared with *hpr1*Δ, we wondered whether this mutation leads to a real impairment in RNAPII transcription, as is the case for *hpr1*Δ strains. First we determined gene expression from *GAL1pr*::*lacZ* and *GAL1pr*::*PHO5* in *hpr1-101* mutant cells compared to wild-type and *hpr1*Δ cells. As shown in Fig. 3A, whereas β-galactosidase activity was clearly diminished in *hpr1-101*, acid phosphatase was not affected. This pattern is similar, although to a lesser extent, to the results obtained for the null *hpr1*Δ strain.

Next, we determined whether the reduction of mRNA levels in *hpr1-101*, as in *hpr1*Δ, was different, depending on the gene tested. We analyzed the mRNA levels in various open reading frames (ORFs) driven by the strong *GAL1* promoter. These ORFs included *lacZ* from *Escherichia coli* (3 kb and 53% GC content); *PHO5* (1.5 kb and 40% GC), *YAT1* (2 kb and 51% GC), and *YRL454* (8 kb and 41% GC) from *S. cerevisiae*; and *LAC4* (3 kb and 41% GC) from *Kluyveromyces lactis*. As shown in Fig. 3B, *hpr1-101* causes a reduction as great as that produced by *hpr1*Δ in the mRNA levels of *lacZ* and *YRL454* but has little effect on *PHO5*, consistent with the enzymatic analysis (Fig. 1). However, it has only a moderate effect on *YAT1* and *LAC4* mRNA levels. These results suggest that the strength of the deficiency in mRNA accumulation in *hpr1-101* cells is also ORF dependent.

In *hpr1*Δ strains, RNAPII processivity, defined as the ability of RNAPII to travel the entire length of a gene, is impaired (23). Although mRNA levels were affected in *hpr1-101*, it was conceivable that RNAPII processivity was not impaired in this strain, therefore separating RNAPII processivity from hyperrecombination. To test this hypothesis, we determined the processivity of RNAPII in *hpr1-101* along the *lacZ* and *YRL454* genes by ChIP. This was performed with an anti-Rpb1 anti-

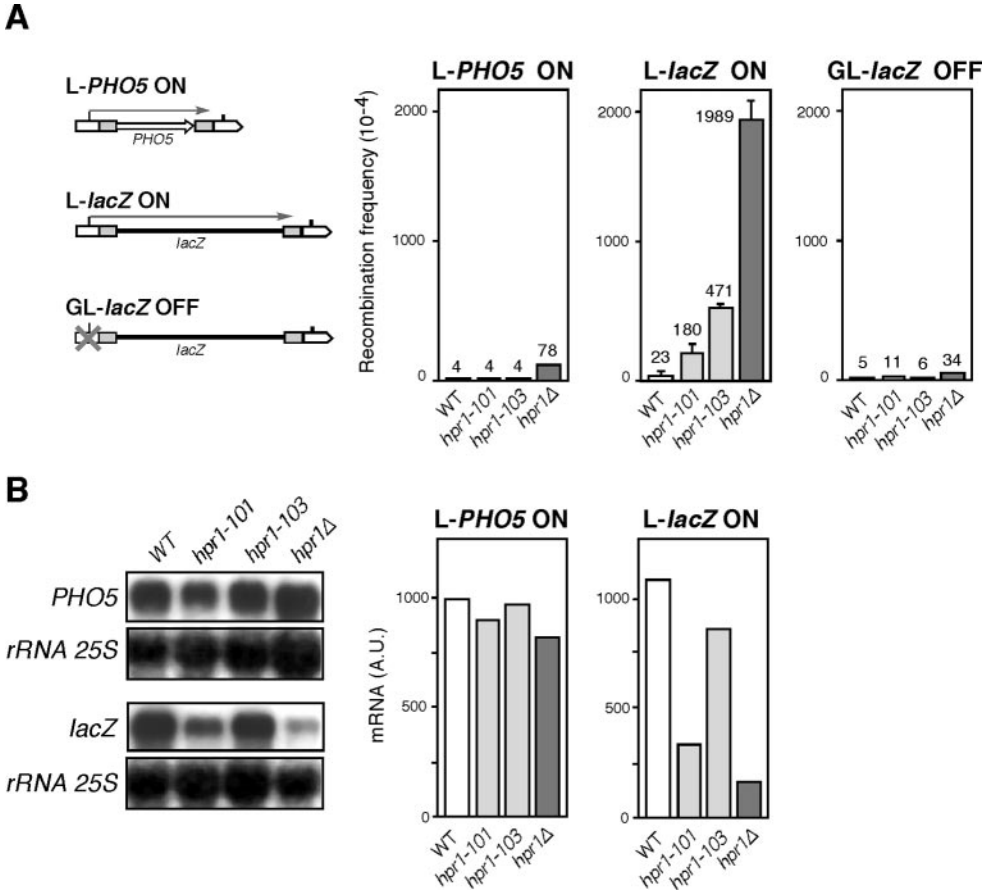

FIG. 2. Recombination in *hpr1-101* and *hpr1-103* mutants. (A) The isogenic strains W303-1A (*WT*), WH101-1A (*hpr1-101*), WH103-1A (*hpr1-103*), and SChY58a (*hpr1*Δ), carrying the mutant alleles integrated in the chromosomal *HPR1* locus, were transformed with plasmid pSCh204 (L-*lacZ* recombination assay) or pSCh206 (L-*PHO5* recombination assay). Gray boxes represent *LEU2* repeats that flank either the *PHO5* or the *lacZ* ORF, as indicated. The white box represents the promoter, and the white solid arrow represents the *CYC* transcription termination site. Shown are recombination frequencies under repressed conditions (glucose) in cells transformed with plasmid pRS314GLlacZ, containing the GL-*lacZ* recombination assay, in which transcription is under the control of the *GAL1* promoter. The recombination frequencies shown are averages of two to four different experiments. (B) Northern analysis of the L-*lacZ* and L-*PHO5* recombination system in isogenic strains W303-1A (WT [wild type]), WH101-1A (*hpr1-101*), and SChY58a (*hpr1*Δ) transformed with either pSCh204 or pSCh206, respectively. Filters were hybridized with either a *lacZ* or a *PHO5* probe and with the 25S rRNA probe. All data were normalized with respect to the rRNA signal. The averages of two experiments are plotted. A.U., arbitrary units.

body and quantitative standard and real-time PCRs at the 5′ end and 3′ end of each coding sequence. As shown in Fig. 4, RNAPII is significantly reduced toward the 3′ end of *lacZ* in *hpr1*Δ, as well as *hpr1-101* (Fig. 4A). In *YRL454*, RNAPII was significantly reduced at the 3′ end in the *hpr1*Δ strain and to a lesser extent in the *hpr1-101* strain (Fig. 4B). These results are consistent with the mRNA accumulation results observed for each gene and indicate that RNAPII processivity is diminished in *hpr1-101*. Thus, we conclude that impaired RNAPII processivity by itself is not sufficient to lead to hyperrecombination. Instead, in *hpr1-103*, RNAPII processivity along *lacZ* was not affected (Fig. 4B), in agreement with the expression data (Fig. 1C), but it was affected for the long (8-kb) *YLR454* ORF to the same extent as in *hpr1-101* (Fig. 4B). This is consistent with the conclusion that *hpr1-103* affects transcription to a minor degree but sufficiently to cause transcription-dependent hyperrecombination.

Nuclear accumulation of poly(A)$^+$ RNA in *hpr1-101* and *hpr1-103* mutants. The transcriptional defect of THO-null mutants such as *hpr1*Δ has been shown to be associated with nuclear accumulation of poly(A)$^+$ RNA caused by defects in mRNA export (19, 40). The functional relationship of THO with mRNA export is provided by the synthetic lethality of RNA export factor mutants in the absence of a functional THO complex, as demonstrated by the *hpr1 mex67-5 ts* double mutants. To explore whether the *hpr1-101* and *-103* point mutants were affected in RNA export, we first determined the capacity of the new mutations to rescue the synthetic lethality of the *hpr1*Δ *mex67-5* mutant. For this, we constructed *hpr1*Δ *mex67-5* strains carrying a *URA3*-based plasmid containing wild-type *HPR1*. These strains were transformed with a plasmid containing either mutant allele *hpr1-101* or *hpr1-103*, and the capacity of each allele to rescue *hpr1*Δ *mex67-5* lethality was determined by growth in SC medium plus 5-fluoroacetic acid (FOA). As shown in Fig. 5A, the ability of each *hpr1* allele to rescue *hpr1 mex67-5* lethality is linked to its transcriptional defect. *hpr1-103*, which had little effect on gene expression, almost completely rescued the synthetic lethality, whereas

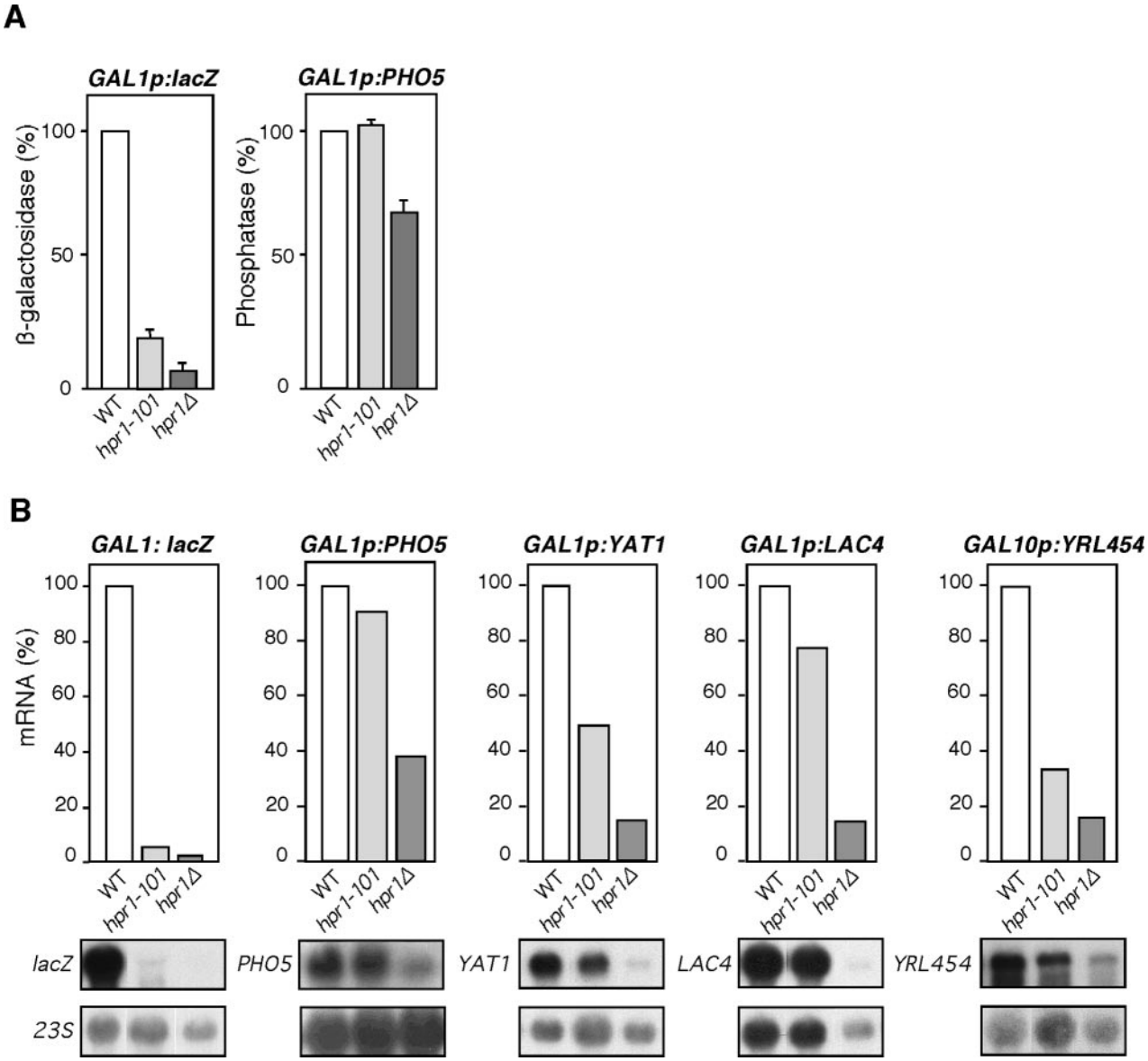

FIG. 3. Transcription analysis of *hpr1-101* versus the wild type and *hpr1*Δ as a function of GC content and the length of the transcribed DNA sequence. (A) Isogenic strains W303-1A (WT [wild type]), WH101-1A (*hpr1-101*), and SChY58a (*hpr1*Δ), carrying the mutant alleles integrated into the chromosomal *HPR1* locus, were transformed with pRS316-GAL1lacZ (*GAL1pr*::*lacZ* fusion) or pSCh202 (*GAL1p*::*PHO5* fusion). β-Galactosidase or phosphatase activity was defined as the percentage (for *lacZ* or *PHO5*, respectively) of the wild-type activity, which was taken as 100%. The mean and standard deviation of three independent experiments are plotted. (B) Northern analysis of mRNA levels in different plasmid constructs containing *lacZ* (pRS416GAL1lacZ), *PHO5* (pSCH202), *LAC4* (pSCH255), and *YAT1* (pSCH247) under the control of the *GAL1* promoter in strains W303-1A (wild type), WH101-1A (*hpr1-101*), and U768-4C (*hpr1*Δ). For the analysis of transcription of the *YLR454* gene, strain WHYL.2A (*hpr1*Δ *GAL1p*::*YLR454*) was transformed with the empty vector YCpA70 (*hpr1*Δ) or with plasmid YCpA13 (*HPR1*) or YCp:hpr1-101 (*hpr1-101*). Others details are the same as those in Fig. 2B.

hpr1-101, which confers strong transcription defects, did not, suggesting a direct correlation between transcription and impaired mRNA export. Analysis of other *hpr1* alleles isolated in this study, such as *hpr1-102* and *hpr1-104*, confirmed this correlation between transcription defect and synthetic lethality with *mex67-5* (data not shown).

We next analyzed the nuclear export of poly(A)$^+$ mRNA by in situ hybridization with a 20-mer oligo(dT) fluorescent probe in the wild-type, *hpr1-101*, *hpr1-103*, and *hpr1*Δ strains (Fig. 5B). Incubation of the cells at 37°C led to nuclear poly(A)$^+$ mRNA accumulation in *hpr1*Δ and *hpr1-101* cells. However, in *hpr1-103* cells, mRNA accumulation was only observed after 6 h of incubation at 37°C. These results indicate that the gene expression defect in *hpr1*Δ and *hpr1-101* cells directly correlates with their mRNA export defect.

Transcription impairment in *hpr1-101* and hyperrecombination in *hpr1-103* are dependent on the nascent mRNA molecule. The transcription impairment and hyperrecombination phenotypes of *hpr1*Δ cells have been shown to be dependent on structures mediated by the nascent mRNA (18). To assay the

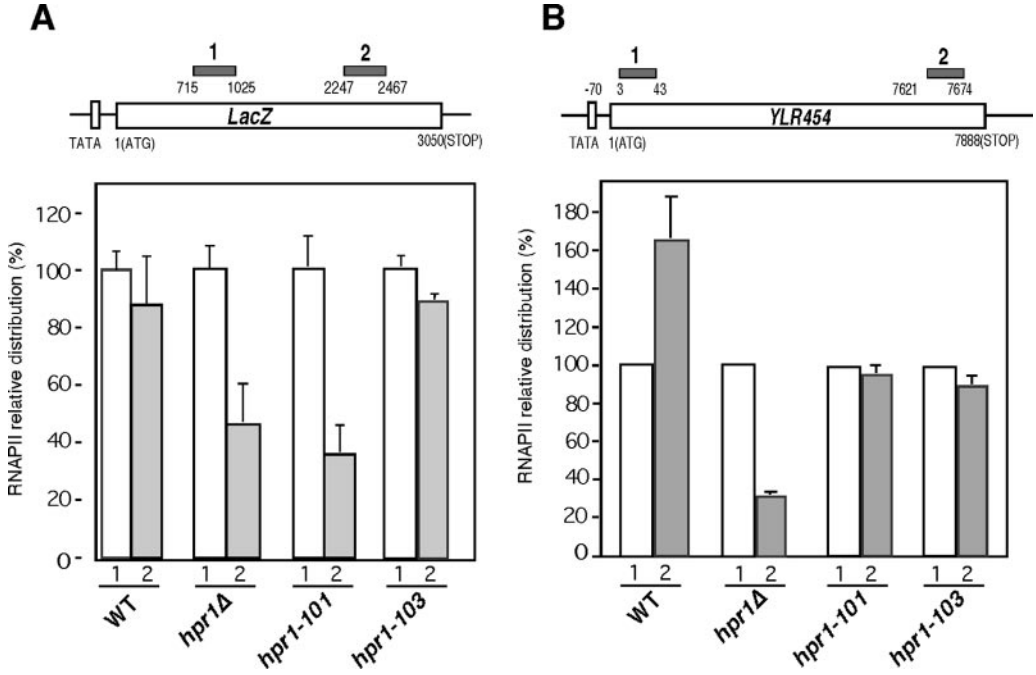

FIG. 4. RNA processivity is affected by *hpr1-101* in a manner strongly dependent on the GC content and moderately dependent on the length of the transcribed DNA sequence. (A) ChIP assays of RNAPII at the *lacZ* gene. Experiments were performed with strains W303 (WT [wild type]), WH101-1A (*hpr1-101*), and U768-4C (*hpr1*Δ) transformed with plasmid pRS416GAL1lacZ containing *lacZ* under the control of the *GAL1* promoter. ChIPs with regions 1 and 2 and an intergenic region as a control were performed in two different transformants, and PCRs were repeated four times for each transformant. The ratio of DNA in regions 1 and 2 was calculated from the DNA amounts in regions 1 and 2 relative to the DNA amount obtained from the intergenic region. Values were normalized to the amount of DNA in region 1 in each strain, which was set to 100% (for details, see Materials and Methods). (B) ChIP assays of RNAPII at the *YLR454* gene under control of the *GAL1* promoter. The experiments were performed with strain WHYL.2A (*hpr1*Δ *GAL1p*::*YLR454*) containing either plasmid YCpA13 (*HPR1*) or YCphpr1-101 (*hpr1-101*) or the empty vector YCpA70 (*hpr1*Δ). ChIPs were performed with two different transformants each, and quantitative PCRs were repeated twice for each transformant. Values were normalized to the amount of DNA in region 1 of each transformant, which was set to 100%.

effect of the nascent mRNA on transcription, we used the previously defined Rib$^+$ and rib^m constructs (Fig. 6A), in which a *PHO5-Rib-lacZ* transcriptional fusion containing either a wild-type (Rib$^+$) or a mutated (rib^m) Hammerhead ribozyme sequence was placed under the control of the *GAL1* promoter (18). In both constructs, a 2.2-kb long mRNA is transcribed, but in the Rib$^+$ construct the active hammerhead ribozyme cleaves the transcript, liberating a 1.8-kb mRNA. Meanwhile, RNAPII travels farther, producing a 0.6-kb mRNA. Northern analysis of the rib^m construct revealed that less transcript was accumulated in *hpr1*Δ and *hpr1-101* cells than in wild-type and *hpr1-103* cells. However, ribozyme cleavage in the Rib$^+$ construct led to an increase in the resulting 0.6-kb transcript so that similar mRNA levels were found in all strains.

Apparently, ribozyme cleavage was capable of increasing the amount of mRNA transcripts in *hpr1*Δ and *hpr1-101* cells. In a previous work, we showed that ribozyme cleavage was capable of partially suppressing the hyperrecombination phenotype observed in *hpr1*Δ cells. Thus, we asked whether ribozyme cleavage might also be sufficient to reduce the hyperrecombination phenotype observed in *hpr1-103* cells. Hyperrecombination was assayed with the GL-Rib$^+$ and GL-rib^m repeat systems containing *PHO5*, followed by active Rib$^+$ or inactive rib^m sequences between 0.6-kb-long *leu2* direct repeats, respectively (Fig. 6B). In the GL-rib^m system, recombination was strongly increased in *hpr1*Δ (285-fold), moderately increased in *hpr1-103* (17-fold), and poorly affected in *hpr1-101* (3-fold). In all three strains, recombination levels were reduced two- to threefold by the ribozyme-mediated cleavage of the nascent mRNA. Therefore, both the transcription defect of *hpr1-101* and the hyperrecombination of *hpr1-103* are similarly dependent on the nascent mRNA, as shown for *hpr1*Δ mutants.

Differential stability and recruitment of the THO complex in *hpr1-101* and *hpr1-103* versus THO-null mutants. The THO complex is a highly stable complex which can be purified with salt concentrations as high as 1.2 M and remains stable in vivo in mutants of the TREX complex such as *sub2*Δ (9, 19). However, the integrity of the THO complex has not been studied in mutants of the THO subunits. To determine whether the different phenotypes of *hpr1-101*, *hpr1-103*, and the THO-null mutants were related to the stability of THO, the complex was purified from the different mutant strains. With a TAP epitope-tagged Tho2 protein, the complex was purified from whole cell extracts derived from wild-type, *hpr1-101*, *hpr1-103*, *hpr1*Δ, *mft1*Δ, and *sub2*Δ strains by two-step affinity purification (19, 33). Western blot analysis with a PAP antibody showed that the amount of TAP-Tho2 was similar in whole cell extracts of *hpr1-101* and wild-type cells (Fig. 7A). Although TAP-Tho2 seems slightly reduced in *hpr1-103* and *sub2*Δ and the amount of Tho2 varies between experiments (Fig. 7A), it was similar in all cases to that in wild-type cells. In contrast, in

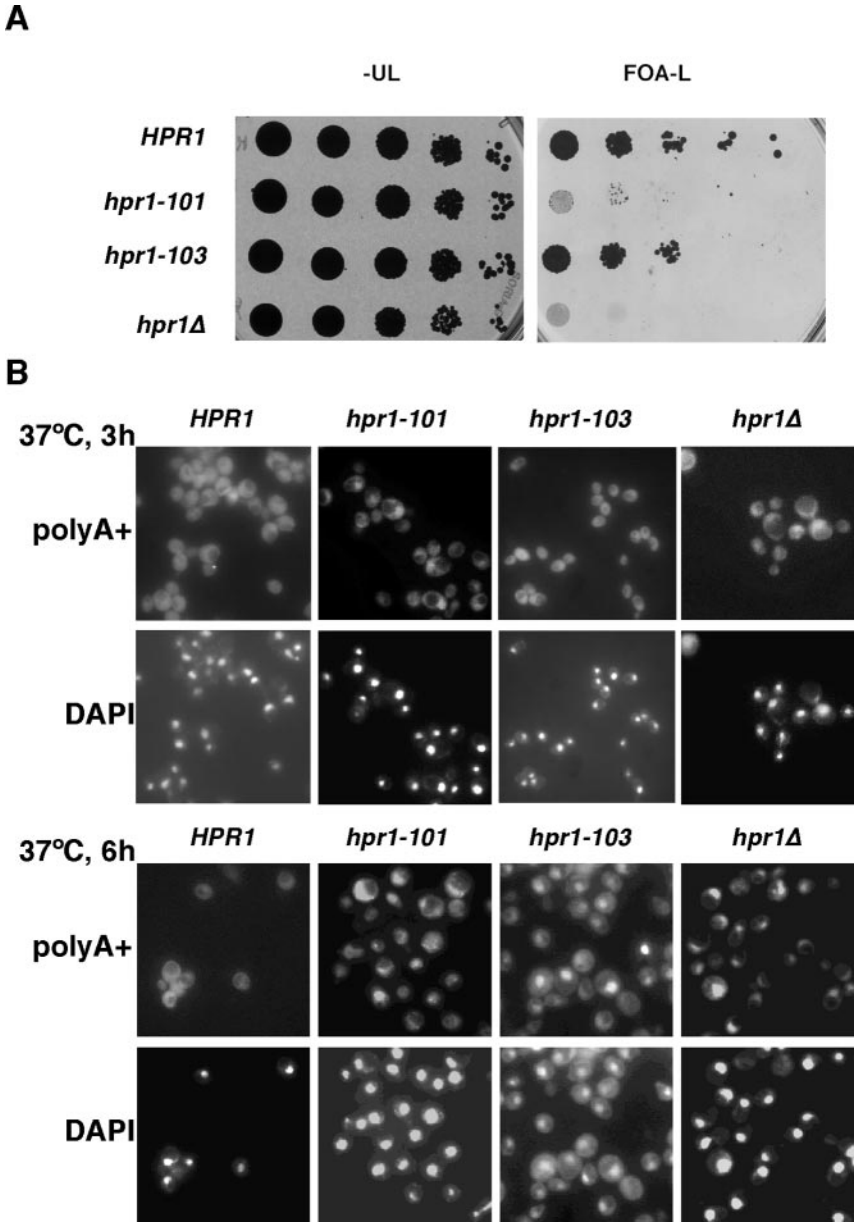

FIG. 5. mRNA export defects of *hpr1* mutants. (A) Suppression of *hpr1*Δ *mex67-5* synthetic lethality. Strain WMH1 (*hpr1*Δ *mex67-5*) transformed with *URA3*-based plasmid pRS316-HPR1 was additionally transformed with *LEU2*-based plasmids YCpA13 (*HPR1*), YCp-hpr1-101 (*hpr1-101*), and YCp-hpr1-103 (*hpr1-103*) or the empty vector YCp70 (*hpr1*Δ). Transformants were spotted in 10-fold serial dilutions on selective medium with or without FOA. Plates were scanned after 3 days of incubation at 30°C. Note that only transformants harboring alleles suppressing the synthetic lethality are able to grow on SC medium-FOA plates. (B) Analysis of nuclear poly(A)$^+$ RNA localization in W303-1A (wild type), WH101-1A (*hpr1-101*), WH103-1A (*hpr1-103*), and U768-4C (*hpr1*Δ) log-phase cultures cultivated for 3 or 6 h at 37°C, as indicated. Samples were immobilized in Teflon-coated slides and hybridized first with a digoxigenin-labeled 20-mer oligo(dT) and second with a fluorescein-conjugated anti-digoxigenin antibody for in situ detection of mRNA. Nuclei were stained with 4′,6′-diamidino-2-phenylindole (DAPI). U, uracil; L, leucine.

*hpr1*Δ and *mft1*Δ, loading of similar amounts of cell extract onto the gel did not permit detection of a signal corresponding to the full TAP-Tho2 protein (Fig. 7A). Only when 10-fold more whole cell extract was loaded was a weak signal corresponding to the TAP-Tho2 protein detectable (Fig. 7A). As *THO2* transcript levels have been found to be similar in wild-type and *hpr1*Δ cells (13), the decrease in Tho2 must result from a posttranscriptional effect, suggesting that THO subunits may only be stable in the form of a complex.

Analysis of the TAP-Tho2 purified THO complex by gradient SDS-PAGE revealed that in the wild type, *hpr1-101*, *hpr1-103*, and *sub2*Δ, the four THO subunits (Tho2, Hpr1, Mft1, and Thp2) were present (Fig. 7B). However, in *hpr1*Δ and *mft1*Δ, only the TAP-Tho2 protein was enriched by the TAP system. Thus, if one of the core proteins of THO is missing, the integrity of the THO complex is greatly reduced. In order to find out whether the remaining proteins form at least some kind of complex, we used an anti-Mft1 antibody to detect

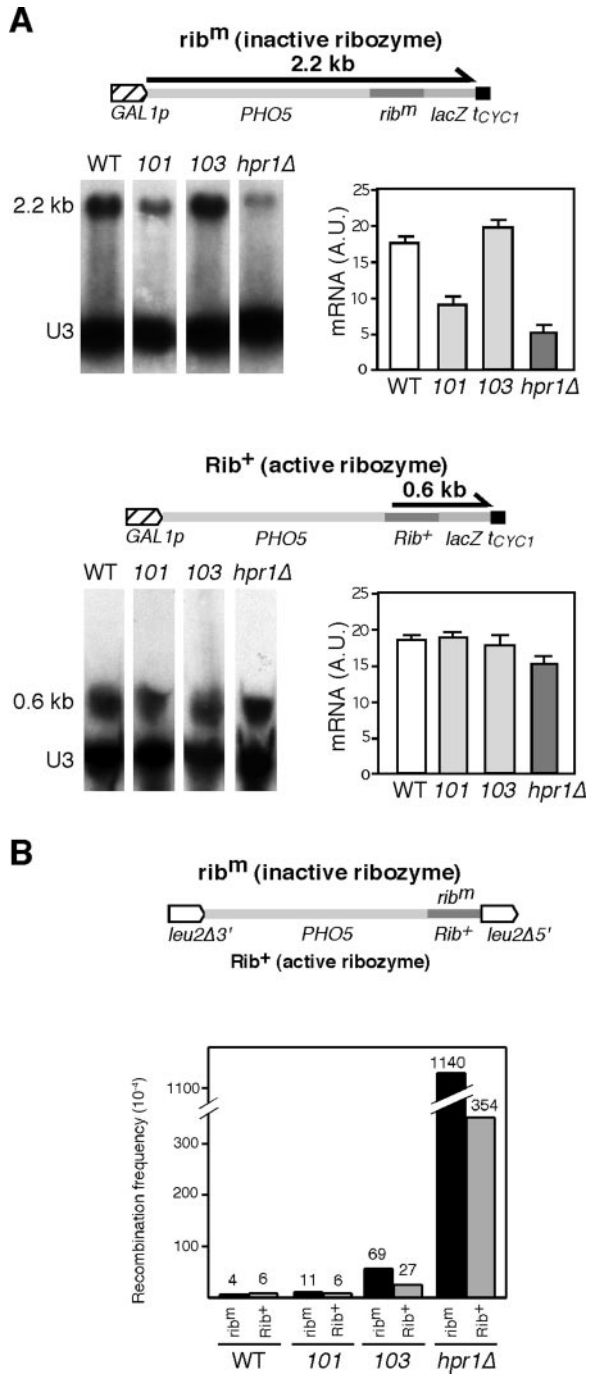

FIG. 6. Nascent-mRNA dependency of the transcription and hyperrecombination defects of *hpr1* mutants. (A) Kinetic analyses of transcription activation of the *rib*^{m} and *Rib*$^+$ fusions in strains W303-1A (WT [wild type]), WH101-1A (*hpr1-101*), WH103-1A (*hpr1-103*), and U678-4C (*hpr1*Δ). The *PHO5-rib*^{m}*-lacZ* (*rib*^{m}) and *PHO5-Rib*$^+$*-lacZ* (*Rib*$^+$) transcriptional fusions were under control of the *GAL1* promoter (*GAL1*$_p$). They contain an active or inactive (respectively), synthetically made, 52-bp ribozyme (*Rib*), followed by a 266-bp fragment of the U3 gene to prevent the cleaved mRNA from degradation and the 369-bp PvuII 3′-end *lacZ* fragment at the untranslated region of *PHO5* (position +1405). Samples were collected 2 h after galactose addition to activate transcription. Electrophoresis was performed with formaldehyde-agarose gels (*rib*^{m}) or urea-acrylamide gels (*Rib*$^+$), and hybridization was with a U3 probe, corresponding to the *rib*^{m} and *Rib*$^+$ region in the scheme. All data were normalized with respect to the endogenous U3 signal. The average of three different experiments is plotted. A.U., arbitrary units. (B) Recombination frequencies of wild-type, *hpr1*, *hpr1-101*, and *hpr1-103* cells containing the recombination systems GL-*Rib*$^+$ (black bars) and GL-*rib*^{m} (gray bars) are shown. Each recombination frequency is the median value of six independent colonies. The average median value of two to four experiments and the standard deviation are plotted.

remaining traces of Mft1 in the TAP-Tho2 purified samples. Similar amounts of Mft1 were detected in wild-type, *hpr1-101*, *hpr1-103*, and *sub2*Δ cells, whereas no signal was detected in *hpr1*Δ and *mft1*Δ cells when similar amounts of TAP-purified Tho2 were loaded (Fig. 7C). However, when 10-fold more Tho2 protein was loaded onto the gel, Mft1 could be detected in *hpr1*Δ TAP-Tho2 purified fractions (Fig. 7C). These results indicate that the THO complex is unstable if one of its components is absent, such as Hpr1 or Mft1, but is stable in both the *hpr1-101* and *hpr1-103* mutants, as well as in mutants in which a TREX component, such as Sub2, is absent.

Since, contrary to *hpr1*Δ, THO is stable in *hpr1-101* and *hpr1-103* cells, we wondered if THO was also recruited into active chromatin in these mutants. With the same TAP-Tho2 strains as before, we found that *hpr1-101* and *hpr1-103* recruited the TAP-Tho2 subunit of THO to a transcriptionally active *PMA1* gene (Fig. 8) at levels clearly above that of *hpr1*Δ mutants. Therefore, the two point mutations analyzed are not null alleles and form THO complexes that are competent for chromatin recruitment.

Sub2 is poorly recruited to active chromatin in both *hpr1-101* and *hpr1-103* mutants. The facts that the presence of THO at the site of transcription elongation helps recruit Sub2 to transcribed chromatin (1, 46) and that multicopy *SUB2* is able to suppress *hpr1*Δ (11, 19) are consistent with the hypothesis that Sub2 recruitment to the nascent mRNA plays a key role in gene expression. As THO is as stable in both *hpr1-101* and *hpr1-103* mutants as in wild-type cells, we wondered whether their respective phenotypes could be caused by different levels of Sub2 recruitment to transcribed chromatin. While testing this possibility, we first noticed that with a *lacZ-URA3* translational fusion under the control of the *tet* promoter (LAUR system) (19), *SUB2* overexpression suppressed the transcriptional defects of both the *hpr1-101* and *hpr1-103* mutants (Fig. 9A). This was consistent with the possibility that Sub2 was not efficiently recruited to transcribed chromatin in both mutants. Again, *hpr1-103* showed a transcription defect in extra-long DNA sequences (Fig. 9A) that reinforces the conclusion that *hpr1-103* is a leaky rather than a separation-of-function mutation.

Sub2 recruitment to active chromatin was directly assayed by ChIP in strains carrying a *SUB2*-TAP epitope fusion at the *SUB2* chromosomal locus with Sepharose IgG and anti-RNAPII antibodies. As shown in Fig. 9B, there was no significant difference in the recruitment of RNAPII to the constitutively transcribed *PMA1* gene between the wild-type and *hpr1* mutant strains tested. Nevertheless, recruitment of Sub2-TAP was as inefficient in *hpr1-101* and *hpr1-103* cells as in *hpr1*Δ cells (55 to 60% of the wild-type level). Therefore, we can conclude that the specific gene expression phenotype of *hpr1-*

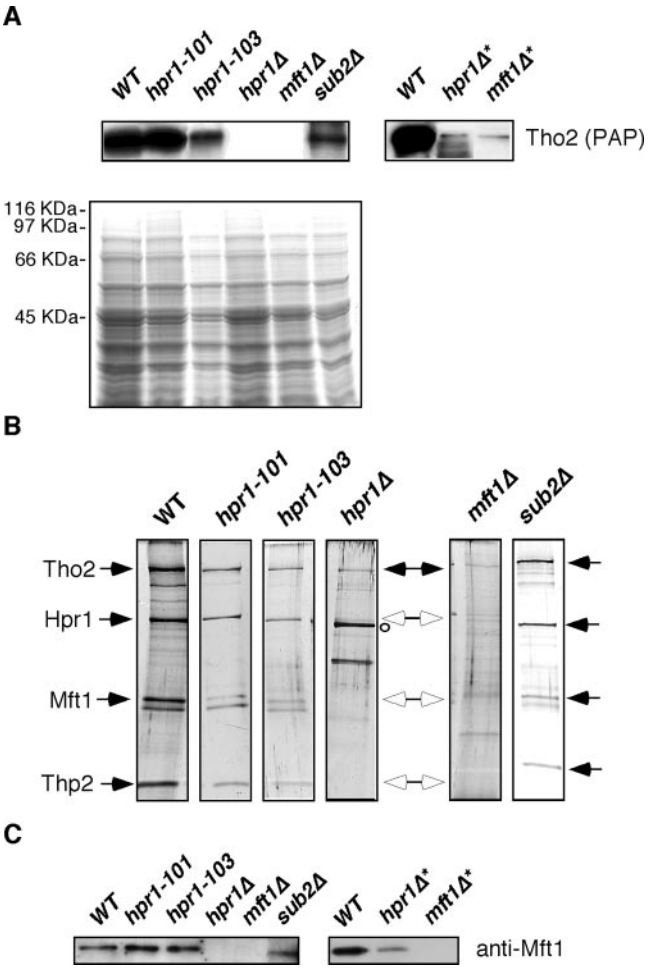

FIG. 7. Analysis of the THO complex in different *hpr1* mutants. (A) Western analysis (top) and Coomassie staining (bottom) of total protein extracts from isogenic strains WWT2T (WT [wild type]), WTT3-4A (*hpr1-101*), WTT4-5C (*hpr1-103*), MTT1 (*mft1*Δ), STT2 (*sub2*Δ), and WTT3-4C (*hpr1*Δ) harboring a Tho2-TAP fusion subjected to SDS-PAGE and hybridized with PAP antibody recognizing the TAP epitope. Either the same amount or a 10-fold excess (marked with an asterisk) of the total proteins shown in the Coomassie-stained gel was loaded for each mutant. (B) Silver-stained gradient SDS-PAGE of purified THO complex from the wild type and *hpr1* mutants. The amount of the eluted fraction loaded in each case was calculated to get the same amounts of TAP-purified Tho2 protein. Arrows indicate the bands corresponding to the four THO subunits (black, detectable; white, nondetectable). The two additional bands observed in *hpr1*Δ strains may correspond to Tho2 degradation products, as suggested by Western analyses (data not shown), but this needs further confirmation. (C) Western analysis of the purified eluted Tho2-TAP fraction subjected to 8% SDS-PAGE and hybridized with anti-Mft1 antibody. Others details are the same as those in panel A. Amounts of protein extracts (marked with an asterisk) similar to those used for panel B or 10-fold excesses were loaded for each mutant.

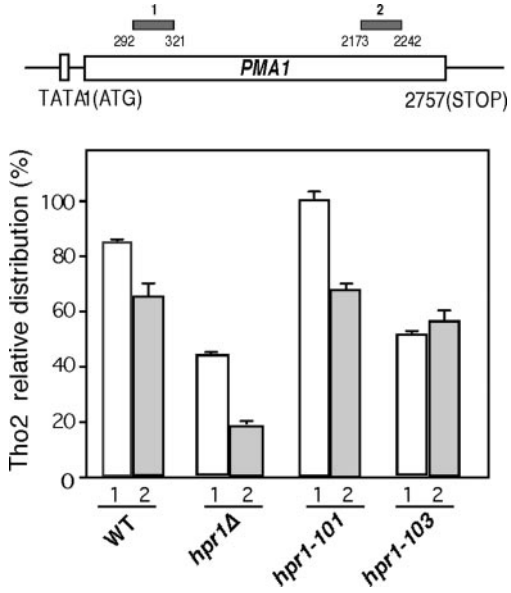

FIG. 8. Recruitment of Tho2 to active chromatin in *hpr1-101* and *hpr1-103* cells, as determined by ChIP analysis of Tho2-TAP to the *PMA1* gene. Experiments were performed with strains WWT2T (W303-1A *THO2-TAP*), WTT3-4A (W303-1A *THO2-TAP hpr1-101*), WTT3-4C (W303-1A *THO2-TAP hpr1*Δ::*KAN*), and WTT4-5C (W303-1A *THO2-TAP hpr1-103*). For each genotype, ChIPs were performed for two different cultures each and quantitative PCRs were repeated twice for each culture. The scheme of the gene analyzed and the DNA fragments amplified by PCR are shown. Other details are the same as those in Fig. 4. WT, wild type.

101 mutants is not caused by different abilities to recruit Sub2 to the nascent mRNA and that inefficient Sub2 recruitment is not enough to trigger either the recombination or the transcription phenotype of *THO* mutants.

Replication fork progression is slowed down in *hpr1-103* but not in *hpr1-101*. We have recently shown that in *hpr1*Δ mutants, hyperrecombination correlates with cell cycle-specific transcription (43). While S-phase-specific transcription was capable of inducing recombination, G_2-specific transcription was not. At the molecular level, replication of the transcribed *lacZ* gene was accompanied with a slowdown of the replication fork during S phase. This slowdown was dependent on both transcription and RNA. We therefore reasoned that the absence of hyperrecombination in *hpr1-101* mutants could be explained if reduced transcription was not associated with slowed-down replication fork progression. To test this possibility, we analyzed replication intermediates of plasmid pRWY005, which contains a replication origin facing the *lacZ* ORF driven by the *GAL1* promoter (Fig. 10A). As shown in Fig. 10B, in contrast to the wild-type intermediates, *hpr1*Δ replication intermediates appear to accumulate around the inflection point (white arrow) and the bubble arc signal gets weaker, indicating a slowdown of fork progression within *lacZ*. However, such an accumulation of simple-Y molecules was not obvious in *hpr1-101* cells, and the intensities of the bubble arc signals were similar in the *hpr1-101* and wild-type strains. In contrast, replication intermediates from *hpr1-103* cells accumulated at the inflection point and toward the 2n spike, although to a lesser extent than in *hpr1*Δ (Fig. 2). These results are consistent with the idea that transcription-associated hyperrecombination of THO mutants is linked to replication fork progression defects (43) and suggest that transcription impairment in *hpr1-101* mutants does not lead to structures capable of slowing down or disrupting replication fork progression. Instead, the mild transcription defect of *hpr1-103* seems to be sufficient to impair replication

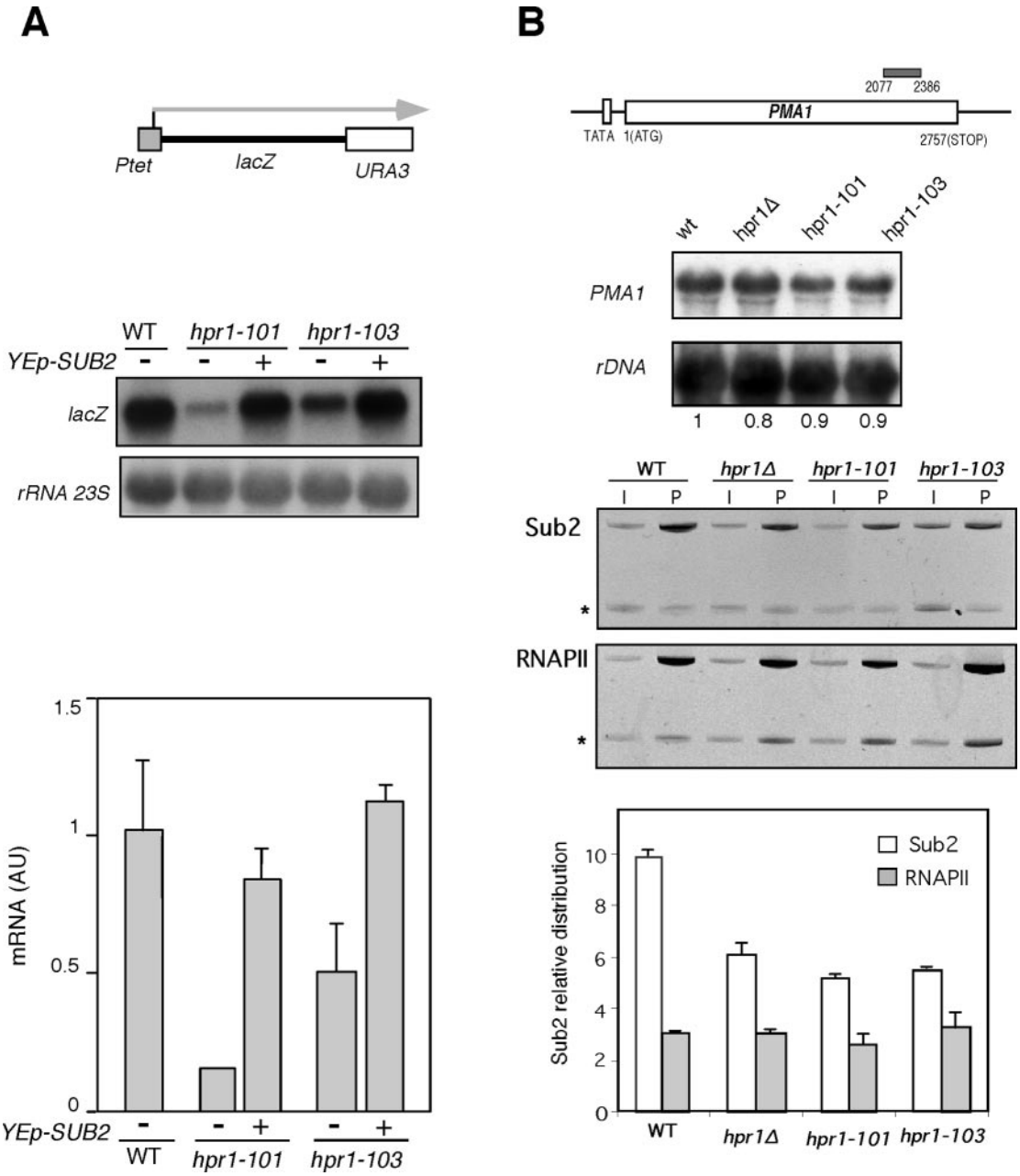

FIG. 9. Recruitment of Sub2 to active chromatin in *hpr1-101* cells. (A) Suppression of the *lacZ* gene expression defect of *hpr1-101* and *hpr1-103* by multicopy *SUB2* as determined by Northern analysis. Strains W303-1A (WT [wild type]), WH101-1A (*hpr1-101*), and WH103-1A (*hpr1-103*) were transformed with pCM184-LAUR containing the *lacZ-URA3* fusion under the control of the *tet* promoter (scheme on top) and with either multicopy plasmid YEp351-SUB2 carrying SUB2 (+) or empty vector YEp351 (−). The experiment was performed in the presence of doxycycline to induce transcription. Others details are the same as those in Fig. 3. (B) ChIP analysis of Sub2-TAP and RNAPII at the *PMA1* gene. The scheme of the genes analyzed and the PCR fragments amplified by PCR are shown at the top, Northern analyses of *PMA1* expression in WT and *hpr1* strains are shown in the middle, and ChIP results are at the bottom. Experiments were performed with strain BSU-S2T-6D (*hpr1*Δ) carrying the chromosomal Sub2-TAP construct and transformed with plasmid YCpA13 (*HPR1*), YCp-hpr1-101 (*hpr1-101*), or YCp-hpr1-103 (*hpr1-103*) or the empty vector YCp70 (*hpr1*Δ). For each genotype, ChIPs were performed with two different transformants each, and PCRs were repeated three times in each case. One representative PAGE gel for each experiment is shown, with the PCR fragment corresponding to the 9716-to-9863 intergenic region of chromosome V used as a control (indicated by an asterisk). The rest of the PCR bands correspond to the specific gene fragments analyzed (see Materials and Methods). The relative abundance of each DNA fragment was calculated as the ratio of each DNA fragment to the intergenic-region quantification results of the precipitated fractions (P) normalized to the corresponding ratios of the input fractions (I).

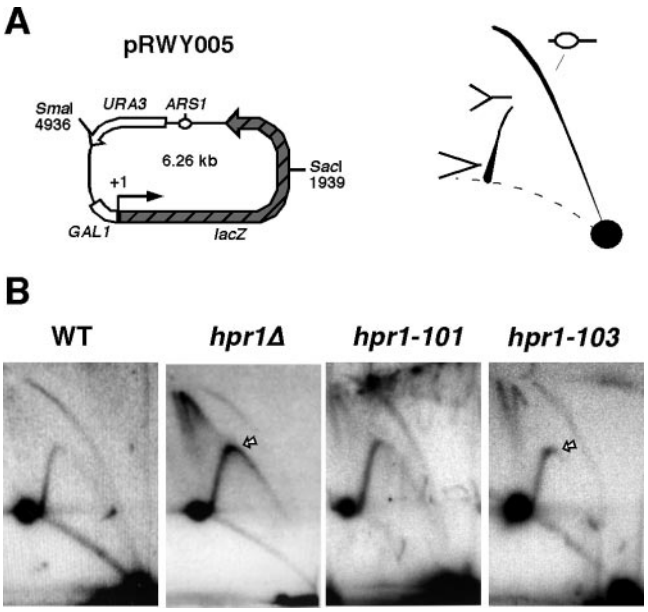

FIG. 10. Replication fork progression in *hpr1-101* and *hpr1-103* cells. (A) Scheme of the 6.26-kb pRWY005 yeast plasmid used for this study (left) and 2D gel pattern of predictable replication intermediates upon plasmid linearization (right). Depicted are restriction sites, functional elements (*ARS1*, open circle; *URA3*, open arrow; *GAL1* promoter, open rectangle; *lacZ* gene, dashed arrow), and shapes of replication intermediates (a bubble and a Y). (B) 2D gel analysis of replication intermediates within a 3.0-kb SacI-SmaI fragment isolated from cells grown in galactose. The replication intermediates were derived from strains W303-1A (WT [wild type]), SChY58a (*hpr1*Δ), WH101-1A (*hpr1-101*), and WH103-1A (*hpr1-103*) transformed with plasmid pRWY005. The inflection point, containing simple-Y molecules of which each arm has approximately the same length (white arrow), is indicated.

fork progression, consistent with its hyperrecombination phenotype.

DISCUSSION

Here we report the isolation and molecular characterization of novel THO complex mutations *hpr1-103*, which produces mutants similar to *hpr1*-null mutants but with weaker phenotypes, and *hpr1-101*, which impairs transcription and RNA export without causing hyperrecombination. As in *hpr1*Δ, the transcriptional defect of *hpr1-101* is dependent on the nascent RNA from highly transcribed long and GC-rich DNA sequences, but it is not sufficient to impair replication fork progression. Therefore, this study indicates that hyperrecombination in all of the THO mutants so far studied is always linked to a transcription defect but that impaired RNAPII processivity alone is not sufficient to induce hyperrecombination as long as replication is not affected. These findings suggest that it is possible to separate the mechanism(s) responsible for mRNA biogenesis defects from the further step of triggering transcription-dependent recombination by THO/TREX dysfunction.

Hyperrecombination requires a threshold level of transcription impairment. Impaired transcription and hyperrecombination are hallmark phenotypes of mutants of the THO complex (Fig. 2). Out of the screen for mutants that allow the dissection of these two phenotypes, *hpr1-103*, together with *hpr1-102* and *hpr-104*, contains multiple point mutations and shows intermediate effects on gene expression and genetic instability, which can be explained by leakiness. Indeed, one of these mutations, *hpr1-102*, is a carboxy-terminal truncation similar to the first, leaky, *hpr1-1* mutation identified (4). Of the three leaky mutants, *hpr1-103* is particularly interesting because of its clear hyperrecombination phenotype and weak effect on transcription. A close look at its phenotypes validates our model in which *hpr1*-mediated hyperrecombination is a consequence of defective transcription. Thus, transcription impairment in *hpr1-103* is detected in DNA sequences such as the *lacZ-URA3* fusion, and RNAPII processivity impairment is detected in long ORFs such as *YLR454*. In the direct-repeat construct (L-*lacZ*) in which hyperrecombination was observed in *hpr1-103*, transcription is also clearly reduced, validating the general conclusion that hyperrecombination in THO mutants is linked to a transcription defect. Indeed, hyperrecombination is only observed in *hpr1-103* when the recombination system is transcribed and depends on the nascent mRNA molecule. Consistently, in *hpr1-103* mutants, recruitment of the Sub2 subunit of TREX to transcribed chromatin is impaired and poly(A)$^+$ RNA is accumulated in the nuclei, although to a lesser extent, as in *hpr1*Δ-null mutants, indicating that *hpr1-103* is also impaired in mRNP formation. The phenotypes of *hpr1-103* are also in agreement with the idea that various kinds of aberrant intermediates could be formed in the presence of a mutated THO complex with different outcomes in transcription and genomic instability. Therefore, the levels of hyperrecombination may not necessarily be proportional to the strength of the transcriptional defect but may reflect the formation of threshold levels of aberrant transcriptional intermediates, such as the RNAPII-DNA-RNA ternary complex, stalled or paused RNAPII, etc.

A nonhyperrecombinant allele, *hpr1-101*, confers the same transcription and RNA export defects as *hpr1*Δ. In contrast to the *hpr1-102* to *-104* leaky alleles, mRNA accumulation of DNA sequences such as *lacZ* in *hpr1-101* cells are strongly reduced, but this is not linked to hyperrecombination. Although a weak increase in recombination is observed in this mutant, the strong gene expression defect, which is similar to that of *hpr1*Δ in *lacZ*, strongly suggests that its major type of transcription defect is not linked to hyperrecombination. The *hpr1-101* mutation probably affects the quality of the mRNP formed as well, and thus its transcription impairment is linked to a synthetic lethality defect in combination with *mex67-5* and a weak mRNA export defect and is dependent on the nascent mRNA molecule. However, our results clearly show that *hpr1-101* cells have a major impairment in transcription elongation, as determined by ChIP, which reflects a defect in RNAPII processivity, as previously shown for *hpr1*Δ (23, 36). Indeed, *hpr1-101* is synthetic lethal with the *spt4*Δ mutant of transcription elongation (data not shown), as also observed for *hpr1*Δ (35). Furthermore, if the low levels of RNA were primarily due to an increased RNA decay in *hpr1-101*, one could predict suppression in cells lacking the Rrp6 3′-5′ exo-RNase subunit of the nuclear exosome. However, *lacZ* mRNA levels remained low in *hpr1-101 rrp6*Δ double mutants (data not shown).

The gene expression defects of *hpr1-101* are similar in in-

tensity to those observed for *hpr1*Δ, including a selective impairment of transcription and a nuclear accumulation of poly(A)$^+$ RNA that are consistent with suboptimal formation of export-competent mRNPs. In favor of this conclusion is the fact that, similar to *hpr1*Δ and *hpr1-103* cells, *hpr1-101* cells are impaired in the ability to recruit Sub2 to transcribed chromatin. Sub2, like its human ortholog UAP56 (37), may be an RNA-dependent ATPase required for the cotranscriptional formation of an export-competent mRNP particle. It functions as a heterodimer together with the Yra1 RNA export factor as part of the TREX complex (39, 40) and is recruited to the transcribed chromatin in a THO-dependent manner (46). Our observation that in *hpr1-101* cells, overexpression of Sub2 suppresses the mRNA accumulation defect as in *hpr1-103* and *hpr1*Δ cells is consistent with the idea that the formation of export-competent mRNPs in *hpr1-101* mutants is caused by their inability to recruit Sub2 properly to the nascent mRNA. This means that in *hpr1-101* mutants, a dysfunctional THO complex incapable of promoting proper mRNP biogenesis and export may be formed. However, the fact that Sub2 recruitment is equally impaired in *hpr1-101* and *hpr1-103*, as well as in *hpr1*Δ, mutants, despite the fact that the intensities of their transcriptional and mRNA export defects are different, strongly suggests that THO has an additional role in mRNP biogenesis, regardless of its capability to help recruit Sub2 into transcribed DNA.

THO constitutes a structural core independent of Sub2 that is unstable in single THO-null mutants but not in *hpr1-101* or *hpr1-103* mutants. An outcome of our work is that THO is a biochemical and functional unit different from Sub2, suggesting that THO may constitute a functional core complex apart from the Sub2-Yra1 heterodimer. Null mutations in presumably all *THO* genes, as shown for *HPR1* and *MFT1*, but not in the Sub2 component of TREX, led to the dissociation of the whole THO complex and the degradation of presumably all THO subunits, as shown for Tho2 (Fig. 7) (19). This could explain the previously reported similarity of phenotypes among the different *THO*-null mutants (9, 40). As the THO complex present in *hpr1-101* and *hpr1-103* is loaded onto active chromatin at similar level as in the wild type, the different gene expression defects of these mutants might be based on distinct interactions between THO and the nascent mRNP or the transcriptional apparatus or on the possibility that THO has several biochemical activities, which would be differentially affected by each point mutation.

The *hpr1-101* allele leads to an L586P amino acid substitution in a well-conserved domain among Hpr1 orthologues from different species from yeast to humans (Fig. 1B). Despite the fact that the biological function of this protein domain in the context of the whole protein is unknown, it seems that this mutation could define a functional motif relevant to the mRNP biogenesis function of THO. Although the change from L to P could introduce a hinge in the protein structure and therefore completely destroy the ability of the protein to interact with other components of THO, our protein purification analysis revealed that this is not the case and that the L residue is essential for its role in mRNP biogenesis and its capacity to facilitate Sub2 recruitment to actively transcribed DNA. The similarity of the phenotypes of *sub2*Δ cells and THO-null mutants (9, 19, 40) suggests that the integrity of a functional THO complex is not sufficient to guarantee proper mRNP biogenesis and export. Our study reveals the need for a functional TREX complex (THO-Sub2, Yra1) at the transcription site for the formation of an export-competent mRNP particle and confirms that THO constitutes a core structural unit apart from Sub2-Yra1. This may be consistent with the facts that, as in *S. cerevisiae* (9), THO has been purified independently of Sub2 in *Drosophila* (32); that humans hHpr1 and hTho2 can be purified apart from UAP56-Aly, orthologues of Sub2-Yra1 (24); and that Sub2 recruitment to active chromatin, contrary to THO recruitment, depends on RNA in yeast (1).

Hyperrecombination of *hpr1* mutants correlates with impaired replication fork progression. The difference in THO integrity between *hpr1*Δ and *hpr1-101* confirms that, despite the strong effect on transcription and mRNA export of *hpr1-101*, the latter is not a null mutation. This conclusion is also clear from the observation that *hpr1-101*, in contrast to all THO-null single mutants, does not lead to hyperrecombination. This nonhyperrecombinant phenotype suggests that in THO/TREX mutants, RNA-dependent transcriptional intermediates resulting from impaired transcription elongation and defective cotranscriptional mRNP formation may not necessarily be sufficient to trigger hyperrecombination. This seems to be the case for *hpr1-101*. Such a nonhyperrecombinogenic intermediate may involve the nascent mRNA, as self-cleavage of the nascent mRNA affected transcript accumulation and recombination rates in all mutants, regardless of whether or not they were hyperrecombinant (Fig. 6) (18). It may be that the nascent RNA is different or that if it is the same, it is insufficient by itself to trigger hyperrecombination. Instead, a further recombinogenic step would be required. Several reports suggest that R loops can be intermediates associated with hyperrecombination in different systems (18, 21, 45). It may be that R loops represent a previous or cooperative step in hyperrecombination and, in addition, an mRNA-RNAPII-DNA tertiary structure able to obstruct replication or the action of a modifying enzyme (such as hAID in class switching), etc., would be required to trigger recombination.

We have recently shown that transcription impairment of *hpr1*Δ along a highly transcribed *lacZ* gene causes a retardation of replication, observed as a slowdown of fork progression (43). This slowdown of fork progression could partially be suppressed by ribozyme-mediated cleavage of the mRNA. As mitotic recombination is a postreplicative DNA repair pathway of, primarily, replication-dependent DNA breaks (25, 26, 34), it seems that in *THO*-null mutants only RNA-dependent transcriptional intermediates that interfere with replication are able to induce recombination. Consistent with this idea, transcription-dependent hyperrecombination in *hpr1*Δ is S phase dependent (43). Indeed, replication is impaired in the hyperrecombinant *hpr1-103* mutant but not in *hpr1-101*, consistent with the idea that hyperrecombination in THO mutants correlates with replication fork impairment.

Different possibilities could explain why, in the absence of a fully functional THO complex, replication fork progression is affected whereas this is not the case in *hpr1-101* cells. One possibility is that elongating RNAPII or another RNA-protein intermediate could be released from the transcription site in wild-type and *hpr1-101* cells via, directly or indirectly, a THO-dependent function still present in Hpr1-101 complexes. Con-

sistently, THO remains stable and seems to be recruited into chromatin in both *hpr1-101* and *hpr1-103* mutants. Further research is required to understand this, and the *hpr1-101* mutation may be a useful tool with which to dissect both the mechanism(s) leading to impaired mRNP biogenesis and the transcription-dependent structure responsible for replication impairment and genomic instability in both THO/TREX mutants and wild-type cells.

In summary, this study indicates that transcription elongation in THO mutants can be impaired without leading to a downstream intermediate at the site of transcription responsible for hyperrecombination, unless such an intermediate impairs replication fork progression. The RNAPII processivity defect in THO mutants may reflect the inability of RNAPII to progress further if mRNP is not properly formed. Whether or not there is a checkpoint mechanism mediated by THO that causes RNAPII to halt or reduce elongation is an attractive possibility to be tested. In this scenario, a further mRNA-dependent step (formation of aberrant mRNA-RNAPII-DNA tertiary structures, etc.) able to impair replication fork progression would be required to cause hyperrecombination. This could be a general feature conserved from bacteria to eukaryotes, as transcription may be an obstacle to replication (28, 41).

ACKNOWLEDGMENTS

We thank H. Gaillard for reading the manuscript, S. Jimeno for providing the Tho2-TAP *mft1*Δ *MTT1* strain, E. Hurt, T. Lithgow, and K. Struhl for kindly providing reagents, and D. Haun for style supervision.

Grants from the Ministry of Science of Education of Spain (BMC2000-0409 and SAF2003-00204) and Junta de Andalucía (CVI102) supported this work. P.H. was the recipient of a predoctoral training grant from the Spanish Ministry of Science and Education.

REFERENCES

1. **Abruzzi, K. C., S. Lacadie, and M. Rosbash.** 2004. Biochemical analysis of TREX complex recruitment to intronless and intron-containing yeast genes. EMBO J. **23:**2620–2631.
2. **Aguilera, A.** 2002. The connection between transcription and genomic instability. EMBO J. **21:**195–201.
3. **Aguilera, A.** 2005. Cotranscriptional mRNP assembly: from the DNA to the nuclear pore. Curr. Opin. Cell Biol. **17:**242–250.
4. **Aguilera, A., and H. L. Klein.** 1990. *HPR1*, a novel yeast gene that prevents intrachromosomal excision recombination, shows carboxy-terminal homology to the *Saccharomyces cerevisiae TOP1* gene. Mol. Cell. Biol. **10:**1439–1451.
5. **Amberg, D. C., A. L. Goldstein, and C. N. Cole.** 1992. Isolation and characterization of *RAT1*: an essential gene of *Saccharomyces cerevisiae* required for the efficient nucleocytoplasmic trafficking of mRNA. Genes Dev. **6:**1173–1189.
6. **Brewer, B. J., and W. L. Fangman.** 1987. The localization of replication origins on ARS plasmids in *S. cerevisiae*. Cell **51:**463–471.
7. **Buratowski, S.** 2005. Connections between mRNA 3′ end processing and transcription termination. Curr. Opin. Cell Biol. **17:**257–261.
8. **Chávez, S., and A. Aguilera.** 1997. The yeast *HPR1* gene has a functional role in transcriptional elongation that uncovers a novel source of genome instability. Genes Dev. **11:**3459–3470.
9. **Chávez, S., T. Beilharz, A. G. Rondon, H. Erdjument-Bromage, P. Tempst, J. Q. Svejstrup, T. Lithgow, and A. Aguilera.** 2000. A protein complex containing Tho2, Hpr1, Mft1 and a novel protein, Thp2, connects transcription elongation with mitotic recombination in *Saccharomyces cerevisiae*. EMBO J. **19:**5824–5834.
10. **Chávez, S., M. Garcia-Rubio, F. Prado, and A. Aguilera.** 2001. Hpr1 is preferentially required for transcription of either long or G+C-rich DNA sequences in *Saccharomyces cerevisiae*. Mol. Cell. Biol. **21:**7054–7064.
11. **Fan, H. Y., R. J. Merker, and H. L. Klein.** 2001. High-copy-number expression of Sub2p, a member of the RNA helicase superfamily, suppresses *hpr1*-mediated genomic instability. Mol. Cell. Biol. **21:**5459–5470.
12. **Fischer, T., K. Strasser, A. Racz, S. Rodriguez-Navarro, M. Oppizzi, P. Ihrig, J. Lechner, and E. Hurt.** 2002. The mRNA export machinery requires the novel Sac3p-Thp1p complex to dock at the nucleoplasmic entrance of the nuclear pores. EMBO J. **21:**5843–5852.
13. **Gallardo, M., and A. Aguilera.** 2001. A new hyperrecombination mutation identifies a novel yeast gene, THP1, connecting transcription elongation with mitotic recombination. Genetics **157:**79–89.
14. **Gallardo, M., R. Luna, H. Erdjument-Bromage, P. Tempst, and A. Aguilera.** 2003. Nab2p and the Thp1p-Sac3p complex functionally interact at the interface between transcription and mRNA metabolism. J. Biol. Chem. **278:**24225–24232.
15. **García-Rubio, M., P. Huertas, S. Gonzalez-Barrera, and A. Aguilera.** 2003. Recombinogenic effects of DNA-damaging agents are synergistically increased by transcription in *Saccharomyces cerevisiae*. New insights into transcription-associated recombination. Genetics **165:**457–466.
16. **Hecht, A., S. Strahl-Bolsinger, and M. Grunstein.** 1999. Mapping DNA interaction sites of chromosomal proteins. Crosslinking studies in yeast. Methods Mol. Biol. **119:**469–479.
17. **Hirose, Y., and J. L. Manley.** 2000. RNA polymerase II and the integration of nuclear events. Genes Dev. **14:**1415–1429.
18. **Huertas, P., and A. Aguilera.** 2003. Cotranscriptionally formed DNA:RNA hybrids mediate transcription elongation impairment and transcription-associated recombination. Mol. Cell **12:**711–721.
19. **Jimeno, S., A. G. Rondón, R. Luna, and A. Aguilera.** 2002. The yeast THO complex and mRNA export factors link RNA metabolism with transcription and genome instability. EMBO J. **21:**3526–3535.

19a. **Jimeno, S., R. Luna, M. García-Rubio, and A. Aguilera.** 2006. Tho1, a novel hnRNP, and Sub2 provide alternative pathways for mRNP biogenesis in yeast THO mutants. Mol. Cell. Biol. **26:**4387–4398.

20. **Kim, M., S. H. Ahn, N. J. Krogan, J. F. Greenblatt, and S. Buratowski.** 2004. Transitions in RNA polymerase II elongation complexes at the 3′ ends of genes. EMBO J. **23:**354–364.
21. **Li, X., and J. L. Manley.** 2005. Inactivation of the SR protein splicing factor ASF/SF2 results in genomic instability. Cell **122:**365–378.
22. **Libri, D., K. Dower, J. Boulay, R. Thomsen, M. Rosbash, and T. H. Jensen.** 2002. Interactions between mRNA export commitment, 3′-end quality control, and nuclear degradation. Mol. Cell. Biol. **22:**8254–8266.
23. **Mason, P. B., and K. Struhl.** 2005. Distinction and relationship between elongation rate and processivity of RNA polymerase II in vivo. Mol. Cell **17:**831–840.
24. **Masuda, S., R. Das, H. Cheng, E. Hurt, N. Dorman, and R. Reed.** 2005. Recruitment of the human TREX complex to mRNA during splicing. Genes Dev. **19:**1512–1517.
25. **McGlynn, P., and R. G. Lloyd.** 2002. Recombinational repair and restart of damaged replication forks. Nat. Rev. Mol. Cell. Biol. **3:**859–870.
26. **Michel, B., G. Grompone, M. J. Flores, and V. Bidnenko.** 2004. Multiple pathways process stalled replication forks. Proc. Natl. Acad. Sci. USA **101:**12783–12788.
27. **Muhlrad, D., R. Hunter, and R. Parker.** 1992. A rapid method for localized mutagenesis of yeast genes. Yeast **8:**79–82.
28. **Prado, F., and A. Aguilera.** 2005. Impairment of replication fork progression mediates RNA polII transcription-associated recombination. EMBO J. **24:**1267–1276.
29. **Prado, F., and A. Aguilera.** 1994. New in-vivo cloning methods by homologous recombination in yeast. Curr. Genet. **25:**180–183.
30. **Proudfoot, N. J., A. Furger, and M. J. Dye.** 2002. Integrating mRNA processing with transcription. Cell **108:**501–512.
31. **Reed, R.** 2003. Coupling transcription, splicing and mRNA export. Curr. Opin. Cell Biol. **15:**326–331.
32. **Rehwinkel, J., A. Herold, K. Gari, T. Kocher, M. Rode, F. L. Ciccarelli, M. Wilm, and E. Izaurralde.** 2004. Genome-wide analysis of mRNAs regulated by the THO complex in Drosophila melanogaster. Nat. Struct. Mol. Biol. **11:**558–566.
33. **Rigaut, G., A. Shevchenko, B. Rutz, M. Wilm, M. Mann, and B. Seraphin.** 1999. A generic protein purification method for protein complex characterization and proteome exploration. Nat. Biotechnol. **17:**1030–1032.
34. **Robu, M. E., R. B. Inman, and M. M. Cox.** 2001. RecA protein promotes the regression of stalled replication forks in vitro. Proc. Natl. Acad. Sci. USA **98:**8211–8218.
35. **Rondón, A. G., M. Garcia-Rubio, S. Gonzalez-Barrera, and A. Aguilera.** 2003. Molecular evidence for a positive role of Spt4 in transcription elongation. EMBO J. **22:**612–620.
36. **Rondón, A. G., S. Jimeno, M. Garcia-Rubio, and A. Aguilera.** 2003. Molecular evidence that the eukaryotic THO/TREX complex is required for efficient transcription elongation. J. Biol. Chem. **278:**39037–39043.
37. **Shi, H., O. Cordin, C. M. Minder, P. Linder, and R. M. Xu.** 2004. Crystal structure of the human ATP-dependent splicing and export factor UAP56. Proc. Natl. Acad. Sci. USA **101:**17628–17633.
38. **Sikorski, R. S., and P. Hieter.** 1989. A system of shuttle vectors and yeast host strains designed for efficient manipulation of DNA in *Saccharomyces cerevisiae*. Genetics **122:**19–27.

39. **Strasser, K., and E. Hurt.** 2001. Splicing factor Sub2p is required for nuclear mRNA export through its interaction with Yra1p. Nature **413:**648–652.
40. **Strasser, K., S. Masuda, P. Mason, J. Pfannstiel, M. Oppizzi, S. Rodriguez-Navarro, A. G. Rondon, A. Aguilera, K. Struhl, R. Reed, and E. Hurt.** 2002. TREX is a conserved complex coupling transcription with messenger RNA export. Nature **417:**304–308.
41. **Trautinger, B. W., R. P. Jaktaji, E. Rusakova, and R. G. Lloyd.** 2005. RNA polymerase modulators and DNA repair activities resolve conflicts between DNA replication and transcription. Mol. Cell **19:**247–258.
42. **Vinciguerra, P., and F. Stutz.** 2004. mRNA export: an assembly line from genes to nuclear pores. Curr. Opin. Cell Biol. **16:**285–292.
43. **Wellinger, R. E., F. Prado, and A. Aguilera.** 2006. Replication fork progression is impaired by transcription in hyperrecombinant yeast cells lacking a functional THO complex. Mol. Cell. Biol. **26:**3327–3334.
44. **Wellinger, R. E., P. Schar, and J. M. Sogo.** 2003. Rad52-independent accumulation of joint circular minichromosomes during S phase in *Saccharomyces cerevisiae*. Mol. Cell. Biol. **23:**6363–6372.
45. **Yu, K., F. Chedin, C. L. Hsieh, T. E. Wilson, and M. R. Lieber.** 2003. R-loops at immunoglobulin class switch regions in the chromosomes of stimulated B cells. Nat. Immunol. **4:**442–451.
46. **Zenklusen, D., P. Vinciguerra, J. C. Wyss, and F. Stutz.** 2002. Stable mRNP formation and export require cotranscriptional recruitment of the mRNA export factors Yra1p and Sub2p by Hpr1p. Mol. Cell. Biol. **22:** 8241–8253.